Available online at www.sciencedirect.com
SCIENCE DIRECT
ELSEVIER
Polymer 46 (2005) 4088–4097
polymer
www.elsevier.com/locate/polymer

Thermosensitive poly(allylamine)-*g*-poly(*N*-isopropylacrylamide): synthesis, phase separation and particle formation

Changyou Gao[a,*], Helmuth Möhwald[b], Jiacong Shen[a]

[a]*Department of Polymer Science and Engineering, Zhejiang University, Hangzhou 310027, China*
[b]*Max-Planck-Institute of Colloids and Interfaces, 14424 Potsdam, Germany*

Received 25 November 2004; received in revised form 20 February 2005; accepted 27 February 2005
Available online 21 April 2005

Abstract

Grafting of poly(*N*-isopropylacrylamide) (PNIPAAm) having carboxylic groups at one end onto poly(allylamine) (PAH) in the presence of water soluble carbodiimide has yielded PAH-*g*-PNIPAAm copolymers with grafting ratios of 50, 29 and 18, respectively. These thermosensitive copolymers exhibit a lower critical solution temperature (LCST) at 34 °C at a temperature increase cycle regardless of their grafting ratios, a temperature identical to that of PNIPAAm-COOH oligomers. Temperature cycling reveals completely reversible polymer aggregation and dissolution above and below the LCST, respectively. Much smaller particle sizes are observed by scanning force microscopy and transmission electron microscopy compared to dynamic light scattering. A porous sphere model is suggested to depict the structure of the particles formed above the LCST, by which the dependence of the particle sizes on their grafting ratios is interpreted taking into account the surface tension and the spatial aggregation distance. Finally, to demonstrate the capability of the copolymers being used as thermosensitive polyelectrolytes, assembly onto multilayers is conducted and the increase of layer thickness is confirmed by small angle X-ray scattering and ellipsometry characterizations.

Keywords: Poly(*N*-isopropylacrylamide); Phase separation; Polyelectrolytes

1. Introduction

Thermosensitive polymers have gained much attention because of their intelligent and reversible behavior in response to environmental stimuli, in particular a temperature variation. Such a behavior, on the one hand, is of great importance for theoretical and basic research, on the other hand, it can be utilized to form intelligent materials with nano or micro dimensions, such as gels, particles, micelles and capsules. These materials in various physical formats have shown intelligent loading and release capabilities for drugs, proteins, nanoparticles, and DNAs under the modulation of temperature, ionic strength, pH values, solvents, and even light, etc. [1–7].

Poly(*N*-isopropylacrylamide) (PNIPAAm), a typical paradigm of thermosensitive polymer, is known to exhibit a lower critical solution temperature (LCST) in aqueous media, below which the polymer is soluble and above which it is in a collapsed phase or water-insoluble [8]. The phase transition of PNIPAAm aqueous solution is understood as a result of dehydration of the polymer chains above the LCST, namely the breakage of hydrogen bonds between amide groups of PNIPAAm and water molecules, thus collapsing the coiled polymer chains into a globular conformation and inducing polymer aggregation at sufficiently high concentration [9–11]. By utilizing this feature and incorporating a crosslinker, such as *N*,*N*′-methylenebisacrylamide into the polymerization system, thermal PNIPAAm hydrogels that exhibit reversible swelling and deswelling have been produced and well studied [1,10,12,13]. Moreover, grafting polymerization of NIPAAm on hydrophobic cores has yielded hairy nanoparticles consisting of thermosensitive hairs, whose hydrodynamic radius was readily tuned by temperature on a scale of hundreds of nanometers [14].

More recently, attention has been paid to copolymers of PNIPAAm and charged polymers (polyelectrolytes), typically poly(acrylic acid), poly(methacrylic acid),

* Corresponding author. Tel.: +86 571 87951108; fax: +86 571 87951948.
E-mail address: cygao@mail.hz.zj.cn (C. Gao).

0032-3861/$ - see front matter © 2005 Elsevier Ltd. All rights reserved.
doi:10.1016/j.polymer.2005.02.115

poly(ethyleneimine), chitosan and etc. [15–18]. A straightforward expectation of such copolymers is that they cannot only respond to temperature, but also pH and other stimuli such as ionic strength. Moreover, the phase transition temperature, strength and sensitivity can all be modulated as well by incorporating charged polymers [15,19–21]. Another feature is that above the LCST the copolymers become amphiphilic, thus can easily form micelles or particles having thermosensitive cores and pH sensitive shells [15,19–21]. Due to the existence of charges on these molecules, block copolymers of PNIPAAm and poly(diallyldimethylammonium chloride) or poly(styrene sulphonate) (PSS) have been assembled into multilayers in a layer-by-layer manner either on planar or curved surfaces [22,23]. After removal of the template cores, hollow microcapsules have been further fabricated [23]. Apparently, the incorporated thermosensitive polymers in thin films or capsules may intelligently gate the permeability and selectivity for some specific molecules or materials [23–25].

Among the polyelectrolytes employed in layer-by-layer assembly so far [26–30], poly(allylamine) (PAH, generally in hydrochloride form) is one of the most frequently adopted since assembly with negatively charged PSS yields always multilayers or hollow capsules with best qualities [31–33]. Driven by this application and also others such as drug loading and release [34,35], we report here the synthesis of PAH-*g*-PNIPAAm obtained from the condensation between PAH and carboxylic end-capped PNIPAAm. The phase transition behavior and capability to form particles above the LCST were determined by dynamic light scattering, scanning force microscopy and transmission electron microscopy. The ability of their assembly onto multilayers was also tested.

2. Experimental section

2.1. Preparation of PAH-g-PNIPAAm

PAH-*g*-PNIPAAm copolymers were synthesized by grafting carboxylic end-capped PNIPAAm (PNIPAAm-COOH) onto PAH chains as shown in Scheme 1. To synthesize the PNIPAAm-COOH polymers, 10 g NIPAAm (88.4 mmol, Aldrich) and 150 mg 4,4′-azobis (4-cyanovaleric acid) (Aldrich, 75%, 0.4 mmol) were dissolved in 50 ml methanol and incubated at 66 °C for 3 h [25]. The solution was then dropped into hot water to precipitate the PNIPAAm-COOH. After washing two times with hot water, the polymers were dissolved in millipore water, and then lyophilized.

Rhodamine 6G (Rd6G) analysis was adopted to quantify the average molecular weight of the PNIPAAm-COOH oligomers, taking acetic acid as a calibration standard [24,36,37]. In brief, 10 mg Rd6G was dissolved in 0.1 M Na_3PO_4 buffer with pH 11, followed by extraction with 100 ml toluene. PNIPAAm-COOH was dissolved in *N*,*N*-dimethylformamide (DMF) to prepare 0.5 mg/ml solution. An equal volume of PNIPAAm-COOH/DMF solution and Rd6G/toluene solution was mixed. After incubation at dark for 30 min, the absorbance spectrum was recorded on a Varian Cary50 Conc UV–visible spectrophotometer. The intensified peak at 536 nm (Fig. 1) was used instead of 515 nm [24] for quantification. A calibration curve was recorded using the same conditions. The molecular weight of the PNIPAAm-COOH oligomers was 2800 supposing that each molecule contains exactly one carboxylic group. A repeated synthesis yielded almost the same molecular weight (2500) of PNIPAAm-COOH (Fig. 1).

To graft the PNIPAAm-COOH (M_w 2800) onto PAH (M_w 65,000), 5% PNIPAAm-COOH aqueous solution was incubated with 1-ethyl-3-(3-dimethylaminopropyl) carbodiimide (EDAC) at 4 °C for 2 days. One gram PAH was then added, and the mixture was incubated for another 2 days before dialysis (cutoff M_w 12,000–14,000) for sufficiently long time. That the dialyzed water became turbid upon heating ensures the successful separation of the unreacted PNIPAAm. The PNIPAAm-COOH/EDAC amounts were varied from 1 g/200 mg, 0.5 g/100 mg to 0.2 g/40 mg to fabricate three PAH-*g*-PNIPAAm samples with different PNIPAAm grafting degrees, which were 50, 29, and 18, respectively, according to elemental analysis. Thus, for brevity the samples were denoted as PAH-*g*-PNIPAAm50, PAH-*g*-PNIPAAm29, and PAH-*g*-PNIPAAm18, respectively.

2.2. Multilayer assembly

To assess the adsorption ability of the copolymers onto negatively charged substrata, 10 layers of PAH/PSS were assembled onto silicone wafers pre-treated with 'piranha' solution. The sequential adsorption of the polyelectrolytes (1.5 mg/ml, in 0.5 M NaCl) was performed by automatically dipping with a Robot. Between alternate exposures to two kinds of polymer solutions for 10 min, there were three rinses with water, each for 3 min. Finally, a layer of PAH-*g*-PNIPAAm copolymers (2 mg/ml, in 0.5 M NaCl) was assembled onto the multilayers having PSS as the outmost layer at 22 °C.

2.3. Characterizations

Elemental analysis regarding C, H and N was carried out with a vario EL elemental analyzer (Analysensysteme GmbH, Germany). Infra red (IR) spectra were recorded on a Nicolet Impact 400. The mass weighted hydrodynamic radius (Rh) as a function of temperature was measured by dynamic light scattering (DLS) on a Malvern High Performance Particle Sizer (HPPS 500). At each temperature the samples were equilibrated at least for 10 min before measurement. All data were averaged from 3 to 5 measurements. The multilayer thickness was measured by ellipsometry (Multiskop from Optrel, Berlin, Germany) at

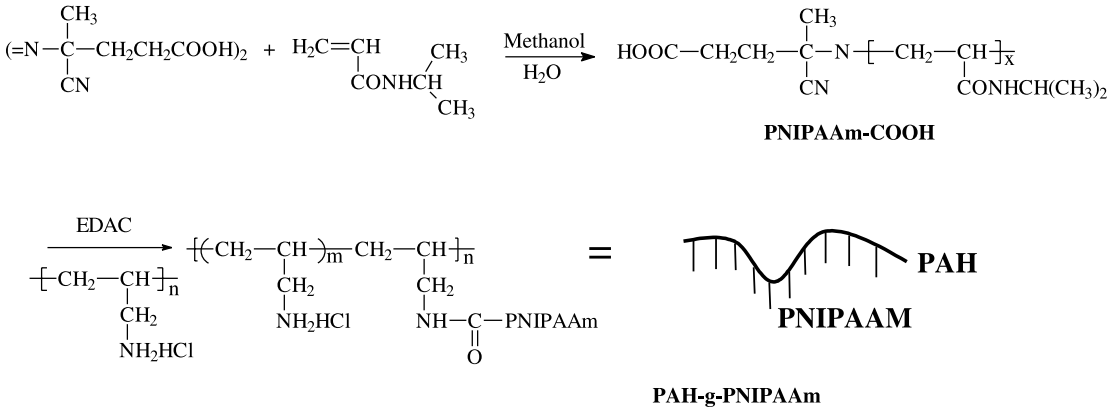

Scheme 1. Synthetic route for PAH-*g*-PNIPAAm.

an incidence angle of 70° and a fixed wavelength of 632.8 nm and small angle X-ray scattering (SAXS, STOE and CIE GmbH, Germany. Cu K_α, $\lambda = 0.154$ nm) at a scattering angle (2θ) ranging from 0.1 to 5.0°. Scanning force microscopy (SFM) images were recorded in air at room temperature (20–25 °C) using a Nanoscope III Multimode SFM (Digital Instrument Inc., Santa Barbara, CA). Transmission electron microscopy (TEM) images were obtained using a Zeiss EM 912 Omega microscope at an acceleration voltage of 120 kV.

3. Results and discussion

3.1. Synthesis of PAH-g-PNIPAAm

In the presence of the carboxylic acid containing initiator, free radical polymerization yielded the thermosensitive polymer with carboxylic groups at one end of the backbone, through which the PNIPAAm is easily grafted onto PAH, catalyzed by the water soluble carbodiimide (Scheme 1) to obtain the copolymer, i.e. PAH-*g*-PNIPAAm. Rd6G analysis confirmed the existence of the carboxylic groups in the PNIPAAm oligomers (Fig. 1), whose molecular weight was 2800. The synthesis was repeated at the same conditions and yielded PNIPAAm oligomers of approximately the same molecular weight (2500).

The weight ratio between PNIPAAm-COOH and PAH was varied to design grafting ratios of 50, 33 and 17%, respectively. IR spectra of the copolymers can be compared with those of the parent components (Fig. 2). In the spectrum of PNIPAAm-COOH, peaks at 1651 and 1541 cm^{-1} are assigned to the typical amide I and amide II, while those at 1458, 1387 and 1367 cm^{-1} are assigned to symmetric and antisymmetric deformation of $-C(CH_3)_2$, respectively, [11]. The amide I (1608 cm^{-1}) and amide II (1506 cm^{-1}) in PAH shifted to lower wavenumbers. All the grafting copolymers showed the typical amides and $-C(CH_3)_2$ absorbance. The bands of amides, however, were shifted with decreasing grafting density, demonstrating that the reaction can thus be followed. Characterization of PNIPAAm-COOH and the copolymers by gel permeation chromatography and ^1H NMR in water did not obtain

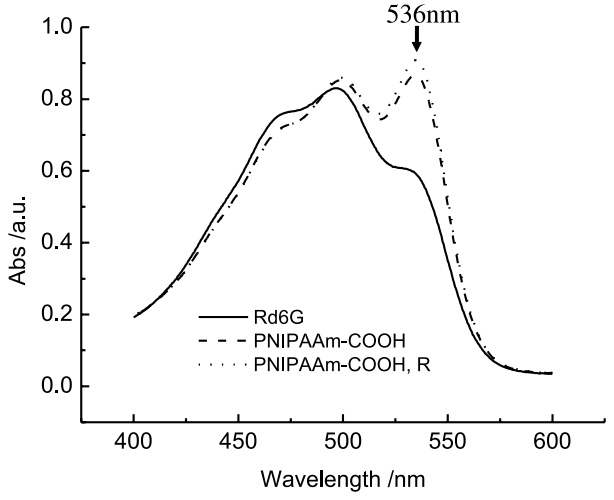

Fig. 1. UV–vis spectra of Rd6G and reaction products of Rd6G and PNIPAAm-COOH. PNIPAAm-COOH, R represents the repeated synthesis under the same conditions.

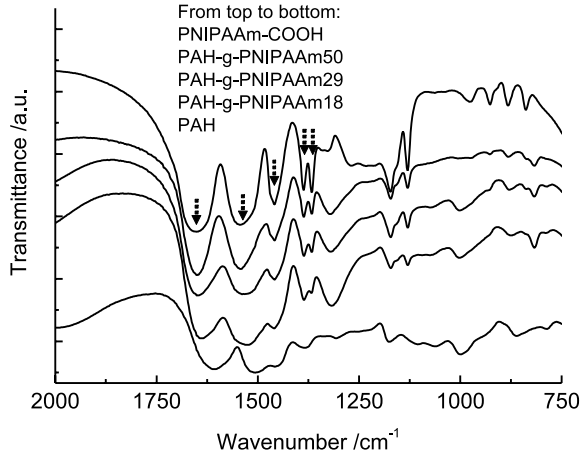

Fig. 2. IR spectra of PAH-*g*-PNIPAAm copolymers with different grafting ratios and of their parent compounds, i.e. PNIPAAm-COOH and PAH.

meaningful results, probably due to the spontaneous formation of particles with sizes of 10–20 nm (see below). Calculation from elemental analysis revealed grafting degrees of 50, 29 and 18%, respectively, which basically match the designed grafting ratios.

3.2. Temperature-induced reversible polymer aggregation

The temperature-induced volume change in aqueous solution is rather typical and well established for PNIPAAm and its copolymers. The phase transition behavior, volume reduction of single polymer coils, and polymer aggregation depend not only on the molecular architecture, concentration, and environmental conditions, but also on the existing forms of the polymers such as freely dissolved in water, anchored on a solid substrate or in a core-shell structure. Copolymerization affects the phase transition temperature in some cases. For example, the incorporation of 5, 10, and 15% of acrylic acid increases the volume phase transition temperature of the PNIPAAm to 40, 50, and 65 °C, respectively, [15,19–21]. In other cases such as core-shell microgels, the copolymerization has almost no influence [15]. To explore the phase transition behavior and the thermosensitivity of the PAH-*g*-PNIPAAm copolymers in aqueous solution, we first measured the hydrodynamic radius (Rh) as a function of temperature by dynamic light scattering (DLS). Fig. 3 presents typical distributions of radii at temperatures below and above the LCST of PAH-*g*-PNIPAAm. At a temperature below LCST such as 30 °C in Fig. 3(a), only one peak centered at 7.2 nm with broader size distribution (relative peak width $\Delta R/R = \pm 0.38$ with weighting on a logarithmic scale) was detected. A slightly larger radius (9.3 nm) and similar relative peak width were observed for PNIPAAm-COOH oligomers at the same temperature. Taking into account the facts that the molecular weight of the PNIPAAm-COOH oligomers was rather small and the radius of PAH was <3 nm (from DLS) at a temperature range of 25–45 °C, the results imply that PNIPAAm-COOH oligomers or PAH-*g*-PNIPAAm copolymers may already self-assemble into nano-particles or micelles. After the temperature was increased to 35 °C, phase separation had occurred as evidenced directly by a change of the solution from transparent to turbid. DLS detected two peaks as showed in Fig. 3(b). The radius of the original particles now shifted to 4.6 nm with a rather narrow relative peak width (± 0.076), while the emerged peak was centered at 159 nm with a relative peak width of ± 0.12. This would mean that one part of the original small particles had accumulated into large ones and the other part remained separately with deswelling caused by dehydration. The shrinkage of the single particle volume was less than four times, a very small value compared with the PNIPAAm hydrogel (~ 15) or PNIPAAm anchored on a particle surface (~ 28) [14]. The reason should be attributed to the charge repulsion contributed by the PAH segments. These values, nevertheless, readily lead to the estimation of the small particle number accumulated in one big particle, which is more than 40,000.

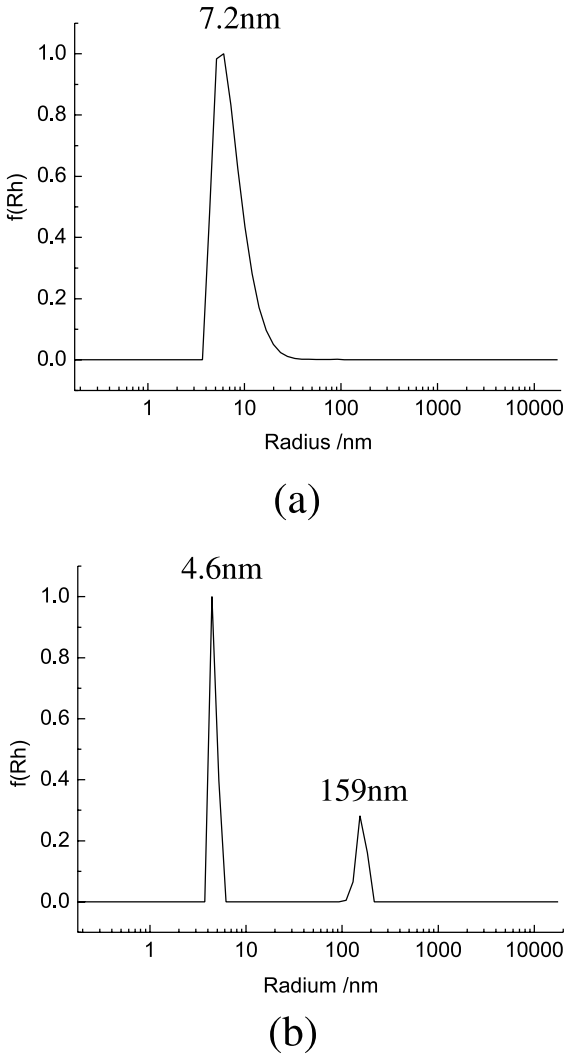

Fig. 3. Typical DLS spectra to show the hydrodynamic radius (Rh) and radius distribution of PAH-*g*-PNIPAAm29 at (a) 30 °C and (b) 35 °C. In (b) part of the original small particles accumulates into large ones to generate the new emerged peak centered at 159 nm. Polymer concentration 0.1 mg/ml in water.

For clarity, in the next discussion we consider only the larger particles after phase separation. Fig. 4 reveals the particle radii during a temperature cycle. For all the polymers, a temperature increase below 33 °C caused a tendency of gradual shrinkage of the small particles, though the extent is minimal compared with the subsequent aggregation. When the temperature increased to 34 °C, phase separation occurred as undoubtedly evidenced by a sudden increase of scattering intensity and particle size increase as a result of polymer aggregation. Interestingly, although the final particle sizes differed largely (Fig. 5), all the polymers of PNIPAAm-COOH and PAH-*g*-PNIPAAm with different grafting ratios had exactly the same phase separation temperature, i.e. 34 ± 1 °C (for brevity, herein we

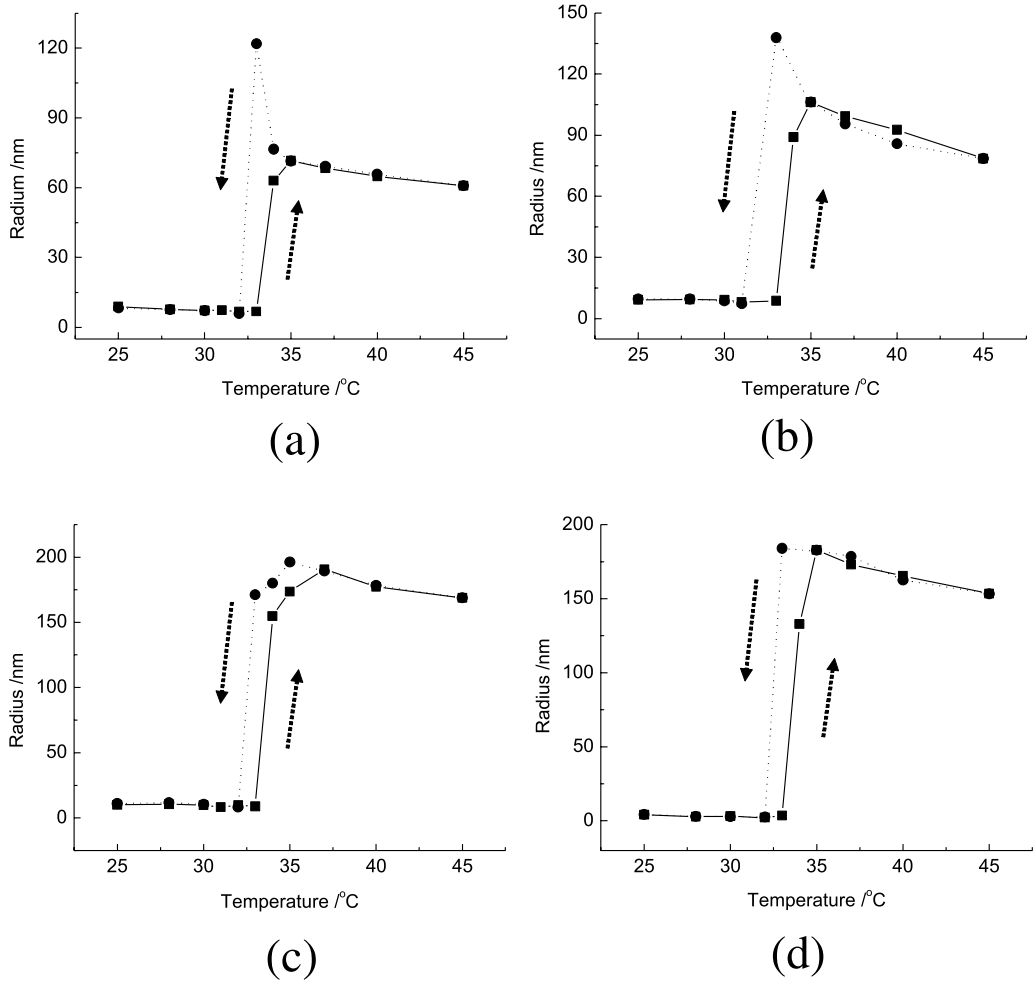

Fig. 4. Hydrodynamic radius as a function of a temperature upon increase and decrease for (a) PNIPAAm-COOH and PAH-*g*-PNIPAAm with grafting ratios of (b) 50%, (c) 29% and (d) 18%. Polymer concentration 0.2 mg/ml in water.

define the emergence of the polymer aggregation point as the LCST). These results imply that a side chain grafting of PNIPAAm does not interfere with the phase separation behavior of the thermosensitive polymers. Similar phenomena have been observed by grafting PNIPAAm onto polyphosphazenes, poly(ethyleneimine) or chitosan [15]. After phase separation, the larger particles of all the samples again exhibited a shrinking tendency along with a temperature increase. An in situ temperature decrease, on the other hand, made the aggregated polymer particles swell and finally be dissolved in water again when the temperature was lower than the LCST. It is worth to note that polymers with a higher PNIPAAm content, e.g. PNIPAAm-COOH and PAH-*g*-PNIPAAm50, exhibited quite a large extent of particle swelling just before dissolution (33 °C) during temperature decrease (Fig. 4(a) and (b)). This swelling completely disappeared when the grafting ratio was lower, i.e. PAH-*g*-PNIPAAm18 (Fig. 4(d)). The higher swelling should be the result of accumulation of water molecules in the particles, forming enough hydrogen bonds with PNIPAAm that are necessary for dissolution. A molecular mechanism might be correlated with entanglement-entanglement interaction as previously described by Lee et al. [for detail, see Ref. [38]]. Since, the polymers of lower grafting ratio have a high enough hydrophilicity and charge

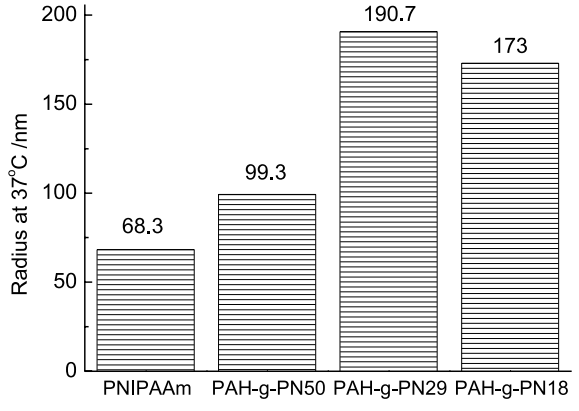

Fig. 5. Hydrodynamic radius at 37 °C at a temperature increase as a function of composition. The inset data represent the radius, respectively. PN is an abbreviation of PNIPAAm.

repulsion ascribed to the PAH backbones, they are easily dissolved without the necessity to experience a large swelling.

Though the introduction of PAH had no influence on the LCST, a dependence of the particle radius on the grafting ratio was found (Fig. 5). Here, we compare the particle radius at 37 °C instead of at 34 °C, the LCST, since at this temperature the particles are far beyond a meta-stable state. Basically, the particle radius increased along with the reduction of the grafting ratio, and reached a maximum value, 190 nm, when the content of PNIPAAm was 29%. A still lower grafting ratio, however, reduced the final particle radius to 170 nm.

Dropping the polymer solutions at 40 °C onto newly cleaved mica to evaporate water fixed the shapes of the particles as explored by SFM measurements (Fig. 6). Fig. 6(a) reveals that the shape of the particles is irregular with an average radius of 18 nm (largest 76 nm) for PNIPAAm-COOH oligomers. Similar sized particles were detected for PAH-*g*-PNIAAm50, yet many small particles were accumulated to form big clusters (Fig. 6(b) and (c)). A few bigger particles with radius of 50–80 nm are also visible. Among all the polymers, PAH-*g*-PNIAAm29 exhibits the best capability to form clearly distinguishable particles (Fig. 6(d) and (e)) of two apparently different radii: 35–40 nm for the larger ones (largest 50 nm) and a few nanometers for the smaller ones (Fig. 3(b)). In contrast to this, no distinguishable particles can be detected for PAH-*g*-PNIPAAm18 but only a homogenous film (Fig. 6(f)), demonstrating that the electrostatic affinity between PAH and the negatively charged mica is so strong that the particles are completely flattened. One has to note that though the absolute sizes are far small detected by SFM compared with DLS, nevertheless a consistent alteration tendency of the particle sizes with DLS can be intuitively concluded except for PAH-*g*-PNIPAAm18.

Taking the in situ dried particles of PAH-*g*-PNIPAAm29 as a typical example, the particles were further characterized by TEM (Fig. 7) to track if their interior is empty or filled. The particles very easily accumulated to form dendrite-like patterns on a cellulose film. Nevertheless, the TEM image indeed provides a proof that the particles are definitely filled other than empty, and their structure is more likely homogeneous instead of a core-shell one.

To develop a model of the structure for the polymer aggregate, it has to be indicated that the PNIPAAm segments are located at sites of PAH backbones in the grafting copolymers (Scheme 1). This molecular structure makes it hard for the copolymers to aggregate in a very condensed core-shell manner as that of block copolymers, due to the strong repulsion arising from the large quantity of ionized NH^{3+} groups. According to the results of DSL, SFM and TEM, however, a porous sphere model would be more suitable as a particle structure at a temperature above the LCST (Scheme 2). Since, the length of the PNIPAAm chains is rather short, the hydrophobic interaction between these chains can only produce hydrophobic phase domains (grey regions) on a very small scale. Accumulation of these domains (because of hydrophobic interaction) in a given spatial volume will then result in a particle having a porous inner structure, with all the interfaces covered by PAH segments. Undoubtedly, the overall surface of the particles should be covered exclusively by the hydrophilic and charged PAH segments. Upon formation of the particles during phase separation, the hydration and particularly the charge repulsion of this 'shell layer' may avoid a further agglomeration of the particles induced by collision, a result of unavoidable Brownian movement. Unfortunately, according to the present results we are unable to describe the fine structure of the grey regions yet, for example, whether they are spherical or not.

To explain the size variation at different grafting ratios, both thermodynamic and hydrodynamic contributions should be considered. Among them, surface tension and the distance for spatial aggregation are most important. A lower grafting ratio of PNIPAAm provides a larger amount of hydrophilic and repulsive components, which may cover a relatively large surface area at a given value of surface tension. Consequently, a larger hydrodynamic radius can be achieved, just like in the case of PAH-*g*-PNIPAAm29. However, at too low grafting ratio the distance of hydrophobic interaction would be rather limited, which again results in aggregation of fewer polymers and a decrease of particle size. It can be extrapolated that no polymer aggregation will take place at an extremely lower grafting ratio, e.g. PAH. Therefore, it is quite reasonable that a maximum radius should appear at a proper grafting ratio, i.e. PAH-*g*-PNIPAAm29 in the present case. That the PNIPAAm-COOH oligomers could also form stable particles above the LCST other than precipitation is most possibly attributed to the hydrophilic and negatively charged carboxylic groups, through which the surface tension between the particles and the bulk water can be effectively balanced and the further particle aggregation is retarded. According to this model, the big difference of radii between DLS and SFM can then be interpreted by particle shrinkage upon removal of the large amount of water content.

At a defined interaction distance in a given spatial volume, lower concentration would mean that fewer polymers will be entangled within the particles upon phase separation. Consequently, the particle size should be smaller. Thus, we further tracked the influence of polymer concentration on the aggregation behavior as a function of temperature increase (Fig. 8). As expected, the size of the particles decreased along with the decrease of polymer concentration above 34 °C, while the phase transition temperature was unchanged. It is worth to note that we have also checked the thermal response of the copolymers with the pH value, yet no influence was found on the LCST.

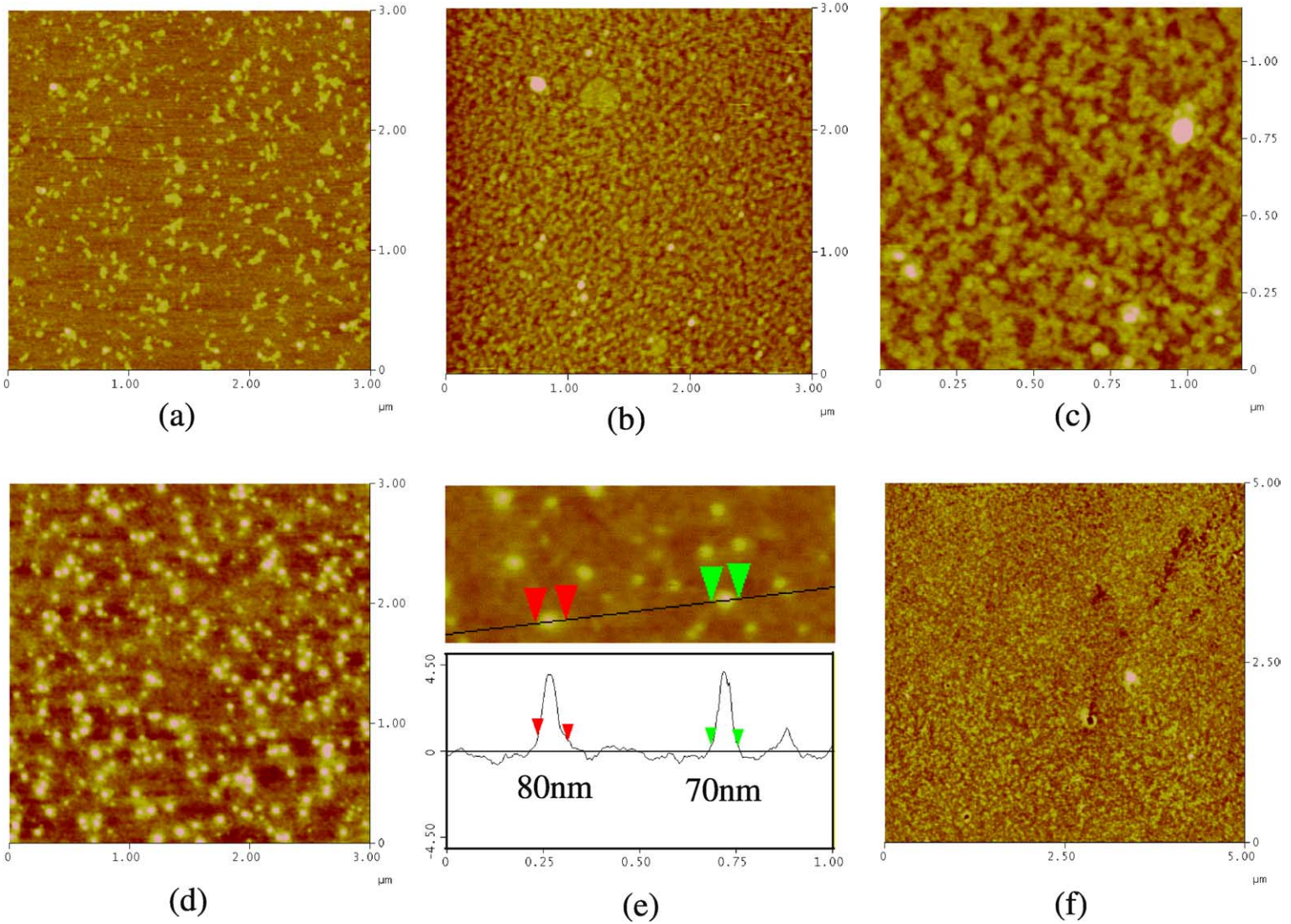

Fig. 6. SFM images to show the morphology of (a) PNIPAAm-COOH, and PAH-*g*-PNIPAAm with grafting ratios of (b), (c) 50%, (d), (e) 29% and (f) 18% dried in situ on mica at 40 °C. The contour plot in (e) corresponds to its upper image. Polymer solutions with a concentration of 0.05 mg/ml are initially incubated at 40 °C for 1 h.

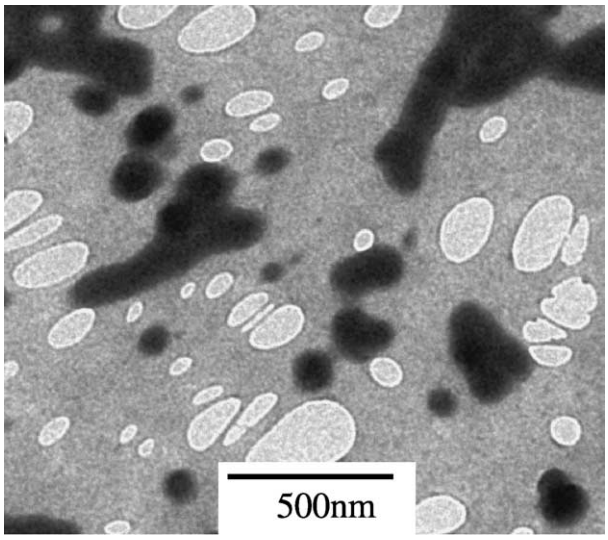

Fig. 7. TEM image of PAH-*g*-PNIPAAm29 dried in situ on a cellulose film at 40 °C from 0.1 mg/ml aqueous solution.

3.3. Assembly into multilayers

As a straight forward application of the copolymers, their capability of interaction with negatively charged polyelectrolytes is essential. To detect this property, we assembled firstly 10 layers of PAH/PSS on silicone wafers, keeping the last layer as negatively charged PSS. Then the silicone wafers were immersed in solutions of the copolymers or PAH. Both SAXS and ellipsometry characterizations confirmed that the copolymers have been successfully assembled onto the multilayers. Compared with PAH, all the copolymers possessed a higher layer thickness (Table 1), apparently due to the extra PNIPAAm in their molecules. This is understandable since the charge density per volume had been decreased. Yet from the much thinner layer thickness (~2 nm) than that derived from the hydrodynamic diameter (~15 nm) of the PAH-*g*-PNIPAAm, one can further deduce that the electrostatic interaction had caused the particles to adjust their globular geometry in solution to form a planar film on the substrate. SFM characterization of the multilayers did not reveal any difference for PAH-*g*-PNIPAAm29 (Fig. 9(c)) and PAH (Fig. 9(a)). Both were very smooth with surface roughness of 0.71 and 0.68 nm at an area of $1\times1\ \mu m^2$ for PAH-*g*-PNIPAAm29 and PAH, respectively. The largest particle size was approximately 30 nm. By contrast, larger grains were found on both PAH-*g*-PNIPAAm50 (Fig. 9(b), largest particle size 30–50 nm) and PAH-*g*-PNIPAAm18 (Fig. 9(d), largest particle size 50–70 nm), whose surface roughness is 0.74 and 1.38 nm, respectively. It is worth to note that these copolymers have also been successfully covered onto polyelectrolyte capsule surface by the present protocol, or assembled into hollow capsules in a layer-by-layer manner with PSS (images not shown).

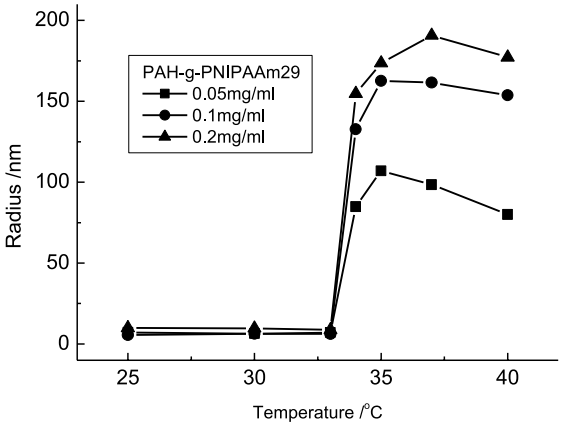

Fig. 8. Temperature dependence of the particle radius of PAH-*g*-PNIPAAm29 for different concentrations.

4. Conclusions

We show here that PAH-*g*-PNIPAAm copolymers have been successfully synthesized by grafting PNIPAAm-COOH oligomers onto PAH backbones. Their molecular structure was characterized by IR spectroscopy and elemental analysis, through which the grafting ratios of three designed samples were quantified as 50, 29 and 18, respectively. A temperature increase and decrease cycle could cause completely reversible polymer aggregation above the LCST and polymer dissolution below the LCST. DLS showed that the PNIPAAm-COOH oligomers and all the PAH-*g*-PNIPAAm copolymers have the same LCST, i.e.

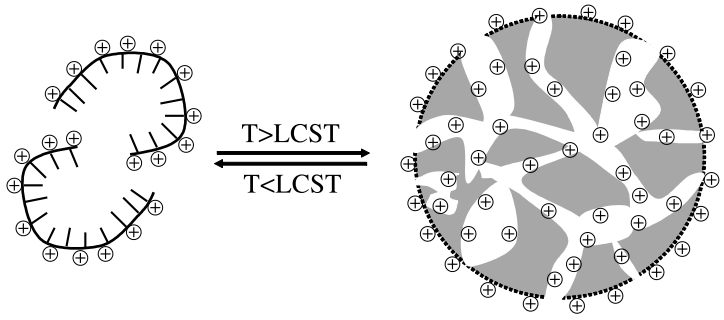

Scheme 2. Schematic illustration to show the particle structure after phase separation.

Table 1
Layer thickness before and after assembly of one layer of PAH or PAH-*g*-PNIPPAm copolymers onto $(PSS/PAH)_5$ multilayers on silicone wafers

Samples	Thickness of $(PSS/PAH)_5$ (nm)	Thickness of $(PSS/PAH)_5$ with one additional layer (nm)	Thickness increment (nm)
PAH	11.9 (13.2)	13.4 (14.1)	1.5 (0.9)
PAH-*g*-PNIPAAm18	11.9 (13.7)	14.2 (15.4)	2.3 (1.7)
PAH-*g*-PNIPAAm29	11.9 (13.1)	13.7 (14.2)	1.8 (1.1)
PAH-*g*-PNIPAAm50	11.9 (13)	14.2 (15)	2.3 (2)

Data were measured from SAXS and ellipsometry (in parentheses).

34 °C at temperature increase, and aggregate into larger particles after phase separation, with sizes depending on composition. Observations under SFM and TEM revealed that the particles were homogeneously filled other than empty, and their sizes were comparatively smaller than that of DLS for all the samples. Based on these results and the molecular architecture of the grafting copolymers, a porous sphere model is suggested to depict the particle structure in aqueous media after phase separation. Due to the rather short length of the PNIPAAm segments and their anchoring at sites of PAH, the formed particle should have a porous inner structure, with its surface and all the interfaces covered by PAH segments. To explain the size variation as a function of grafting ratio, we further suggest that surface tension and spatial aggregation distance should be taken into consideration. Finally, these PAH-*g*-PNIPAAm copolymers

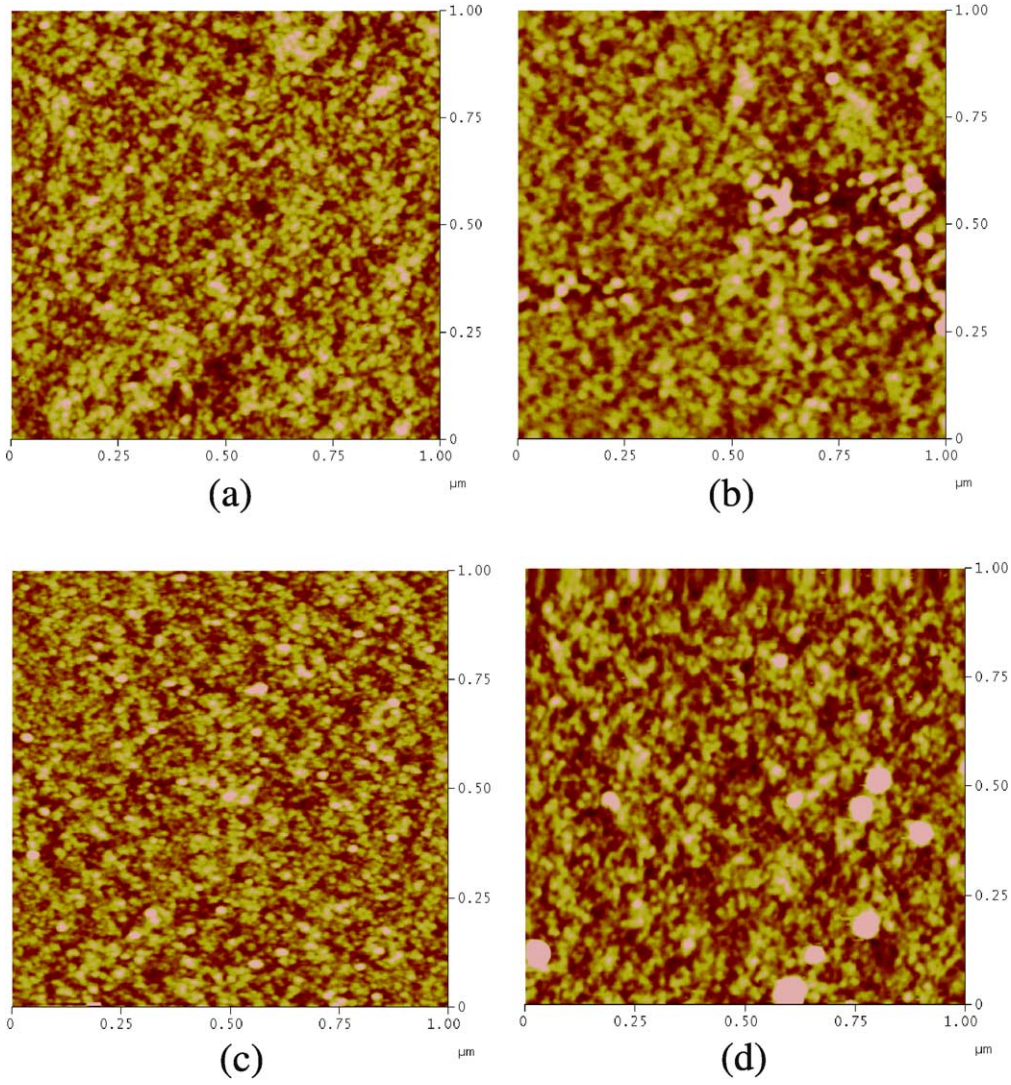

Fig. 9. SFM images of 10 layers of PAH/PSS multilayers on silicone wafer after assembly with an additional layer of (a) PAH, and PAH-*g*-PNIPAAm with grafting ratios of (b) 50%, (c) 29% and (d) 18%.

were assembled onto multilayers, demonstrating their capability of being used as thermosensitive polyelectrolytes.

Acknowledgements

We thank H. Zastrow, A. Heilig, W. Dong, S. Liu, S. Pyrok, J. Hartmann and R. Pitschke for their assistance on DLS, SFM, SAXS, ellipsometry, elemental and TEM measurements. C. Gao thanks the Max-Planck Society for a visiting scientist grant. This study is financially supported by the Natural Science Foundation of China (No. 20434030 and 90206006) and the National Science Fund for Distinguished Young Scholars of China (No. 50425311).

References

[1] Ito K, Chuang J, Alvarez-Lorenzo C, Watanabe T, Ando N, Grosberg AY. Prog Polym Sci 2003;28:1489.
[2] Buchholz BA, Doherty EAS, Albarghouthi MN, Bogdan FM, Zahn JM, Barron AE. Anal Chem 2001;73:157.
[3] Kurisawa M, Yokoyama M, Okano T. J Controlled Release 2000;69: 127.
[4] Kurisawa M, Yokoyama M, Okano T. J Controlled Release 2000;68: 1.
[5] Liu XM, Pramoda KP, Yang YY, Chow SY, He CB. Biomaterials 2004;25:2619.
[6] Kang SI, Na K, Bae YH. Colloids Surf, A 2003;231:103.
[7] Chaw CS, Chooi KW, Liu XM, Tan CW, Wang L, Yang YY. Biomaterials 2004;25:4297.
[8] Liu XM, Wang LS, Wang L, Huang JC, He CB. Biomaterials 2004; 25:5659.
[9] Annaka M, Amo Y, Sasaki S, Tominaga Y, Motokawa K, Nakahira T. Phys Rev E 2002;65 [Art. No. 031805].
[10] Annaka M, Motokawa K, Sasaki S, Nakahira T, Kawasaki H, Maeda H, et al. J Chem Phys 2000;113:5980.
[11] Maeda Y, Higuchi T, Ikeda I. Langmuir 2000;16:7503.
[12] Wu SN, Li H, Chen JP, Lam KY. Macromol Theory Simul 2004;13: 13.
[13] Cheng SX, Zhang JT, Zhuo RX. J Biomed Mater Res A 2003;67A:96.
[14] Takataa S, Shibayamaa M, Sasabeb R, Kawaguchib H. Polymer 2003; 44:495.
[15] Leung MF, Zhu JM, Harris FW, Li P. Macromol Rapid Commun 2004;25:1819.
[16] Bokias G, Staikos G, Iliopoulos I. Polymer 2000;41:7399.
[17] Sotiropoulou M, Cincu C, Bokias G, Staikos G. Polymer 2004;45: 1563.
[18] Gupta V, Nath S, Chand S. Polymer 2002;43:3387.
[19] Dong LC, Hoffman AS. J Controlled Release 1991;15:141.
[20] Kratz K, Hellweg T, Eimer W. Colloids Surf, A 2000;170:137.
[21] Yoo MK, Sung YK, Lee YM, Cho CS. Polymer 1998;39:3703.
[22] Steitz R, Leiner V, Tauer K, Khrenov V, Von Klitzing R. Appl Phys A-Mater 2002;74:S519.
[23] Glinel K, Sukhorukov GB, Mohwald H, Khrenov V, Tauer K. Macromol Chem Phys 2003;204:1784.
[24] Kidchob T, Kimura S, Imanishi Y. J Controlled Release 1998;50:205.
[25] Park YS, Ito Y, Imanishi Y. Langmuir 1998;14:910.
[26] Decher G. Science 1997;277:1232.
[27] Decher G, Hong JD. Makromol Chem Macromol Symp 1991;46:321.
[28] Keller SW, Johnson SA, Brigham ES, Yonemoto EH, Mallouck TE. J Am Chem Soc 1995;117:12879.
[29] Decher G, Lehr B, Lowack K, Lvov Y, Schmitt J. Biosens Bioelcetron 1994;9:677.
[30] Ruths J, Essler F, Decher G, Riegler H. Langmuir 2000;16:8871.
[31] Donath E, Sukhorukov G, Caruso F, Davis S, Möhwald H. Angew Chem Int Ed 1998;37:2201.
[32] Gao CY, Moya S, Lichtenfeld H, Casoli A, Fiedler H, Donath E, et al. Macromol Mater Eng 2001;286:355.
[33] Gao CY, Donath E, Möhwald H, Shen JC. Angew Chem Inter Ed 2002;41:3789.
[34] Li XW, Huang YS, Xiao J, Yan CH. J Appl Polym Sci 1995;55:1779.
[35] Kitano H, Yan CH, Nakamura K. Makromol Chem-Macromol Chem Phys 1991;192:2915.
[36] Ito Y, Kotera S, Inaba M, Kono K, Imanishi Y. Polymer 1990;31: 2157.
[37] Ito Y, Inaba M, Chung DJ, Imanishi Y. Macromolecules 1992;25: 7313.
[38] Lee NK, Abrams CF, Johner A, Obukhov S. Phys Rev Lett 2003;90 [Art. No. 225504].